Implementation of Permanent Magnet Synchronous Motor Fault Diagnosis by a Stacked Autoencoder

I-His Kao, Wei-Jen Wang, I-Chieh Chiang, and Jau-Woei Perng, *Member, IEEE*

ABSTRACT

This manuscript presents an effective diagnosis algorithm for permanent magnet synchronous motors running with an array of faults of varying severity over a wide speed range. The fault diagnosis is based on a current signature analysis. The complete fault motor diagnosis system requires the extraction of data based on the proposed method, and a subsequent method for adding classifications. In this paper, we propose a feature extraction method using a stacked autoencoder and a classification method using a softmax layer. The results show that the proposed methods can effectively diagnose five different motor states, including two different demagnetization fault states and two bearing fault states.

INTRODUCTION

Several studies have employed time-domain analysis to diagnose faulty motors. In [1], a fast and accurate motor condition monitoring and early fault detection system was developed using one-dimensional convolutional neural networks. The experimental results obtained using real motor data demonstrated the effectiveness of the proposed method for real-time motor condition monitoring. In this study, we present a feature extraction method using a stacked autoencoder with a softmax layer to classify permanent magnet synchronous motor (PMSMs) into five states. The experimental results show that our proposed methods can effectively diagnose five different motor states running at speeds of 150–3,000 RPM.

PMSM FAULT SIGNAL

A. Normal PMSM

We measured the current time-domain signal of a normal motor. The signal is composed of sine wave combinations, and the period of each sine wave is the period for which the driver operates the motor. Furthermore, by observing the changes in the size of each peak, we can see that the magnetic distribution is not perfect. Connecting all the peaks reveals that the peak connection is a sinusoidal waveform, and not a horizontal line. However, there is an acceptable tolerance for the amount of magnetization present.

B. Demagnetization Faults in PMSM

In our experiments, we utilized two types of demagnetization fault, each with a different degree of demagnetization. One demagnetization fault was created by replacing one of the permanent magnets in the rotor with an aluminum magnet of equal weight (aluminum has no magnetic properties). This method ensures that the balance of the motor dynamics is not affected, preventing eccentricity failures. A second demagnetization fault was created by reducing the magnetic flux of one of the permanent magnets by half. We refer to this as a semi-demagnetization fault for the remainder of this paper.

By measuring the demagnetization fault, we find that the demagnetization phenomenon leads to a non-sinusoidal component in the current signal. Therefore, nearby waveforms are also affected. The current signal for the motor with a demagnetization fault is significantly different from the current signal generated by the normal motor. Using high- and low-frequency harmonics that are close to the main frequency, the frequency of the fault feature can be determined as in [2]:

$$f_{dmg} = f_s(1 \pm k/p),\ \mathrm{k} = 1,2,3,\ldots, \tag{1}$$

where f_{dmg} is the fault feature frequency, f_s is the electrical angular frequency, and p is the number of pole pairs in the rotor. By observing the motor with a semi-demagnetization fault, we determined that the peaks of this motor are relatively small.

C. Bearing Fault in PMSM

According to [3] and [4], the relationship between the bearing eccentricity and electrical angular frequency is defined by

$$f_{bng} = \left|f_s \pm m f_{i,o}\right|, \tag{2}$$

where $f_{i,o}$ is related to the specification of the bearing by

$$f_{i,o} = \frac{n}{2} f_r \left[1 \pm \frac{db}{pd}\cos\beta\right], \tag{3}$$

where m is a positive integer, n is the number of balls in the bearing, $f_{i,o}$ is the feature vibration frequency, f_r is the mechanical angular frequency, *db* is the diameter of the ball, and *pd* is the diameter of the raceway.

In the experiments, motors with two types of bearing faults were examined. The faults were located at different parts of the bearing. One of the bearing faults was designed to simulate a bearing inner ring that has been damaged by metal fatigue in the form of raceway cracks. The processing method used a drill on the inner ring to create four small holes. These holes are symmetrical, in order to maintain the rotational balance. The second bearing fault was designed to simulate a bearing raceway produced in a factory environment, where it was subjected to a large amount of fine iron powder. The processing method involves removing the bearing and adding soft aluminum powder to the raceway. The motor was subjected to higher friction during rotation, but no sound or vibration can be directly observed.

When observing the motor with the first type of bearing fault (damaged by drilling the inner ring), as the ball struck the borehole, the disturbance current caused the waveform to turn slightly at the crest. However, it is not easy to observe the difference between this type of motor and the normal motor.

When observing the other type of bearing fault (bearing raceway filled with aluminum powder), the increase in rotor friction caused the amplitude of the stator current to slightly

increase. Because there is less noise when this type of motor is running, it is difficult to diagnose faults using a microphone. In the stator current of this type of motor, the harmonic distribution differs from that of the demagnetization fault. However, the amplitude of the motor with the bearing fault is not as obvious as the amplitude of the motor with the demagnetization fault. Therefore, we can infer that the two bearing faults have not yet strongly affected the smooth operation of the motors.

STACKED AUTOENCODER STRUCTURE

In this paper, we propose an unsupervised learning method called stacked autoencoder (SAE). An autoencoder is an artificial neural network used for unsupervised learning. The functionality of an SAE is very similar to that of a principle component analysis. The aim of an autoencoder is to learn a representation for a set of data, typically for the purpose of dimensionality reduction. Recently, the autoencoder concept has been more widely adopted for learning generative models of data [5] [6].

Because an autoencoder can be divided into two parts, the first consisting of the encoder and decoder and the second being the middle of an overlapping code layer, the model input is from the encoder and the output is the decoder output. Furthermore, the encoder comprises the feature extraction of the input, while the output can fit the input of the autoencoder. The difference between a stacked and traditional autoencoder is the number of layers. An SAE includes a deep artificial neural network.

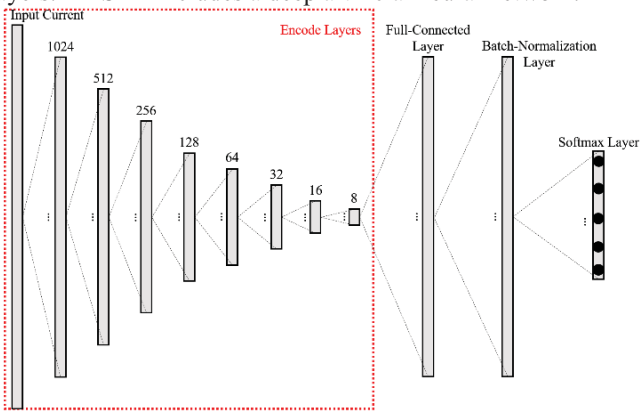

Fig. 1. Diagram of the encode layer with a softmax layer.

The input layer consists of 2000 sample points of the time domain signal. Our SAE architecture generally has eight encode layers and eight decode layers. The encode layer with a softmax layer is illustrated in Fig 1. The Adam with the mean square error function is used to train the parameters of the SAE model.

EXPERIMENT

From the fast Fourier transform spectrum, we can verify whether there is an aliasing effect within the 1 kHz spectrum. While observing high-frequency components, there may be some information in the >1 kHz spectrum. To avoid generating a large amount of redundant data, we selected the sampling rate as 2 kHz for the system specifications. However, this sampling rate also covers the electrical angular frequency of the lowest 10 Hz of the time information. Thus, we selected 2,000 samples per second for the fault diagnosis system specifications.

We can calculate the accuracies of different methods, as listed in Table 1.

Table 1 Diagnosis Accuracy of the Methods

Methods	NM	DFM	SDFM	DIRM	APM	Total
WPT	88.5%	88%	87%	89%	91%	88.7%
SAE	**99%**	**97%**	**92%**	**99%**	**95%**	**96.4%**

Here, HNM is the diagnosis accuracy of the normal motor, DFM is the diagnosis accuracy of the demagnetization fault motor, SDFM is the diagnosis accuracy of the semi-demagnetization fault motor, DIRM is the diagnosis accuracy of the damaged inner ring motor, and APM is the diagnosis accuracy of the aluminum powder motor. We also compare our method with a traditional feature extraction method, wavelet package transform (WPT). It is seen that the diagnosis accuracy rate of the SAE is considerably higher than that of the WPT.

CONCLUSION

The stator current signals of motors with demagnetization and semi-demagnetization faults, whether in the time domain or frequency domain, are highly similar. In addition, the waveforms from motors with a damaged inner ring or aluminum powder are very similar, regardless of the domain. Although it is considerably difficult for humans to classify the five types of motors, our proposed systems can efficiently classify them with an accuracy of 96.4%. Although training the systems requires a high-specification PC, the testing does not need such computational power. While the motor driver detects the stator currents of PMSMs, we can diagnose PMSMs at any time while they are spinning.

REFERENCES

[1] T. Ince et al., "Real-time motor fault detection by 1-D convolutional neural networks," *IEEE Trans. Ind. Electron.*, vol. 63, no. 11, pp. 7067-7075, Nov. 2016.

[2] S. Nandi, H. A. Toliyat, and X. Li, "Condition monitoring and fault diagnosis of electrical motors-a review," *IEEE Trans. Energy Convers.*, vol. 20, no. 4, pp. 719-729, Dec. 2005.

[3] M. E. H. Benbouzid, "A review of induction motors signature analysis as a medium for faults detection," *IEEE Trans. Ind. Electron.*, vol. 47, no. 5, pp. 984-993, Oct. 2000.

[4] J. R. Stack, R. G. Harley, and T. G. Habetler, "An amplitude modulation detector for fault diagnosis in rolling element bearings," *IEEE Trans. Ind. Electron.*, vol. 51, no. 5, pp. 1097-1102, Oct. 2004.

[5] M. B. Lazreg, M. Goodwin, and O. C. Granmo., "Vector representation of non-standard spellings using dynamic time warping and a denoising autoencoder," in *IEEE Congress on Evolutionary Computation*, Donostia, San Sebastián, Spain, Spain, 2017, pp. 1444-1450.

[6] F. Lv, M. Han, and T. Qiu, "Remote sensing image classification based on ensemble extreme learning machine with stacked autoencoder," *IEEE Access*, vol 5, pp. 9021-9031, May 2017.